Multireference Configuration Interaction Study on the Potential Energy Curves and Radiative Lifetimes of Low-Lying Excited States of CdH+ Cation

ARTICLE *in* CHEMICAL PHYSICS · OCTOBER 2014

Impact Factor: 1.65 · DOI: 10.1016/j.chemphys.2014.09.003

8 AUTHORS, INCLUDING:

Xiaomei Zhang
Jilin University
11 PUBLICATIONS **13** CITATIONS
SEE PROFILE

Rui Li
Jilin University
14 PUBLICATIONS **32** CITATIONS
SEE PROFILE

Xue-Shen Liu
Jilin University
77 PUBLICATIONS **484** CITATIONS
SEE PROFILE

Bing Yan
Jilin University
47 PUBLICATIONS **63** CITATIONS
SEE PROFILE

Chemical Physics 443 (2014) 142–148

Contents lists available at ScienceDirect

Chemical Physics

journal homepage: www.elsevier.com/locate/chemphys

Multireference configuration interaction study on the potential energy curves and radiative lifetimes of low-lying excited states of CdH^+ cation

Xiaomei Zhang, Guiying Liang, Rui Li, Dandan Shi, Yuchen Liu, Xueshen Liu, Haifeng Xu *, Bing Yan *

Institute of Atomic and Molecular Physics, Jilin University, Changchun 130012, China
Jilin Provincial Key Laboratory of Applied Atomic and Molecular Spectroscopy (Jilin University), Changchun 130012, China

ARTICLE INFO

Article history:
Received 16 July 2014
In final form 6 September 2014
Available online 16 September 2014

Keywords:
CdH^+
MRCI + Q
Spin–orbit coupling
Spectroscopic constant

ABSTRACT

Ab initio calculations on CdH^+ cation have been performed with the high-level relativistic MRCI + Q method. The potential energy curves of seven low-lying Λ–S states, correlated with the dissociation limits $Cd^+(^2S_g) + H(^2S_g)$, $Cd(^1S_g) + H^+(^1S_g)$, and $Cd^+(^2P_u) + H(^2S_g)$, are computed. And the accurate spectroscopic constants of the bound Λ–S are determined. The permanent dipole moments (PDMs) of Λ–S states as well as the spin–orbit matrix elements are evaluated. The results indicate that the abrupt changes of PDMs and the spin–orbit matrix elements are attributed to the change of the electronic configurations at the avoided crossing point. After considering the spin–orbit coupling (SOC) effect, the 12 Ω states generated from the Λ–S states are investigated. It is indicated that the SOC effect is substantial for CdH^+, leading to the double-well potential of $(3)0^+$ state. Finally, the transition properties of several transitions are reported, including the transition dipole moments, Franck–Condon factors, and radiative lifetimes.

1. Introduction

Because of their great importance as intermediates in many chemical reactions, for example, homogeneous hydrogenation, hydroformylation, hydrometallation and transfer hydrogenation, transition metal hydrides have attracted considerable interest during the past several decades [1–3]. The investigations on the low-lying electronic states of these molecules, to retrieve accurate structural and spectroscopic constants as well as to reveal the dynamics and interaction of the states, are of significant value to understand the detailed reaction mechanisms. Comparing to neutral transition metal hydrides, which have been extensively studied both by spectroscopic techniques and theoretical calculations [4–20], the knowledge about the cations is rather sparse. Generally, it could be more difficult to produce clean and abundant cation source for spectroscopic measurement. An accurate prediction provided by high-level calculations is thus required to understand the properties of the electronic states of the cations of transition metal hydrides.

This paper focuses on the low-lying electronic states of cadmium hydride cations, CdH^+, which could be likely a carrier in the global cycling of toxic cadmium [21,22]. Experimental spectroscopic constants of CdH^+ are only available for the ground state $X^1\Sigma^+$ [23,24] and the first excited singlet state $A^1\Sigma^+$ [23], which were reported more than 40 years ago by using spectrograph. On the other hand, many theoretical efforts have been performed in the literature using various calculation methods, such as relativistic and non-relativistic Hartree–Fock [25,26], configuration interaction (CI) with effective core potential (ECP) [27], Generalized Valence Bond (GVB) method [28], relativistic Fock-space coupled-cluster [29], and recently, multi-configuration second-order perturbation theory (CASPT2) method with ANO-RCC basis set [30]. All the theoretical studies reported to date are focused on the ground electronic state $X^1\Sigma^+$ of CdH^+, from which the equilibrium bond distance, the vibrational and rotational constants as well as the dissociation energy have been derived. However, the calculated results of the $X^1\Sigma^+$ state by different theoretical methods exhibit relatively large discrepancy. Further studies with high-correlated theoretical method are still in demand. Particularly, the spin–orbit coupling (SOC) effect, which has not been considered in the previous calculations of CdH^+, could have significant effect on the shape of the potential energy curves (PECs) of electronic states, especially for the molecules containing heavy atoms. Regarding the electronic excited states of CdH^+, to the best of our knowledge, there are unfortunately no theoretical studies available in the literature.

In the present work, high-level relativistic multi-reference configuration interaction with Davidson correction (MRCI + Q) study

* Corresponding authors at: Institute of Atomic and Molecular Physics, Jilin University, Changchun 130012, China. Tel.: +86 431 85168817; fax: +86 431 85168816.
E-mail addresses: xuhf@jlu.edu.cn (H. Xu), yanbing@jlu.edu.cn (B. Yan).

http://dx.doi.org/10.1016/j.chemphys.2014.09.003
0301-0104/

on the ground as well as the low-lying excited states of CdH^+ are carried out. The PECs of the 7 Λ–S states associated with three lowest dissociation limits of CdH^+, as well as those of 12 Ω states generated from the Λ–S states after considering the SOC effect, were computed. Based on the calculated PECs, the spectroscopic constants for the bound states were obtained, most of which have not been reported previously. The transition properties and the interaction between different electronic states via the SOC effect were also discussed for the first time. The electronic configurations compositions in Λ–S wavefunctions and compositional variations of Λ–S components in Ω wavefunctions were examined and used to interpret the electronic and transition properties of CdH^+. The calculation presented here will provide more comprehensive results about the structure and behavior of the low-lying electronic states of CdH^+.

2. Calculation method

The whole ***ab initio*** calculations on the electronic structure of CdH^+ cation were performed via the quantum chemistry MOLPRO 2010 program package [31]. The spectroscopic constants of $^{114}CdH^+$ were determined with the aid of the LEVEL 8.0 program [32]. It should be mentioned that the effect of the isotope on spectroscopic results is very small because of large atomic mass and could be ignored in our results.

The single-point energy calculations were carried out to obtain the potential energy curves (PECs), where the contracted Gaussian-type all-electron augmented correlation consistent basis sets aug-cc-pwCVTZ-DK [33] are selected for atoms Cd and aug-cc-pV5Z-DK [34] for H in the calculations.

In order to obtain the high-level PECs of CdH^+, the potential energies at a set of bond lengths are calculated by adopting the following three steps: first, the restricted Hartree–Fock (RHF) method is selected to produce the single-configuration wavefunction of the ground state. Then, the multi-configuration wavefunction is calculated with the state-averaged complete active space self-consistent field (SA-CASSCF) method [35,36]. Finally, the internally contracted multi-reference configuration interaction (MRCI) approach [37,38] is employed to launch the correlation energy calculation and achieve the accurate energies based on the acquired optimized reference wavefunction in the SA-CASSCF calculation. At the same time, the calculation is extended to include the relativistic effect in order to improve the level of the PECs, where the one-electron integral second-order Douglas-Kroll integrals is used to evaluate the Scalar relativistic effect [39]. Adding a Davidson correction (+Q) balances the size-consistency error of MRCI method. The potential energy curves (PECs) of these 7 Λ–S electronic states are drawn with the help of the avoided crossing rule of the same symmetry.

Because of the limit of the MOLPRO program, C_{2v} point group symmetry, the subgroup of the $C_{\infty v}$ point group, is adopted in the calculation of electronic structures, which holds A1/B1/B2/A2 irreducible representations. For CdH^+, 3a1, 1b1 and 1b2, the symmetry molecular orbitals (MOs) are determined as the active space, which corresponds to the atoms Cd 5s5p and H 1s shells. The outermost $5s^1$ electrons of Cd^+ and $1s^1$ electrons of H are placed in the active space. Through our testing, 4d orbital in the active space would lead to much time-consuming but not bring much improvement to the spectroscopic results. The more suitable plan is that the 18 electrons of 4s4p4d shell are placed in the closed shell. These orbitals are doubly occupied in all reference configuration state functions, and correlated via single and double excitations. That is, there are totally 20 electrons of CdH^+ used in the calculation of electronic correlation energy.

After the MRCI calculation, the spin–orbit coupling (SOC) effect is taken into consideration via the state interaction approach with the Breit–Pauli Hamiltonian operator (H_{BP}) and the mean-field one-electron Fock operator [40]. In the SOC calculation, the MRCI + Q energies of Λ–S state as well as the MRCI wavefunctions are employed to calculate the SO matrix. Thus, the energies of the Ω states are obtained by the diagonalization of the calculated SO matrix. The SOC effect makes the 7 Λ–S electronic states split into 12 Ω electronic states. The rearranged potential energy curves are plotted with the aid of the avoided crossing rule of the same symmetry.

Based on the PECs of the Λ–S and Ω electronic states, the spectroscopic constants, including equilibrium internuclear distance R_e, excitation energy T_e, vibrational constants ω_e and $\omega_e\chi_e$, balanced rotation constant B_e, are determined by numerical solution of the one-dimensional nuclear Schrödinger equation. The dissociation energy D_e is obtained by subtracting the molecular energy at R_e from the energy at a large separation. The TDMs of several transitions from excited $\Omega = 0^+$ and 1 states to the $X0^+$ state are also calculated and the Franck–Condon factors are evaluated by the LEVEL8.0 program. Finally, the radiative lifetimes of the selected transitions are calculated.

3. Results and discussion

3.1. The PECs and spectroscopic constants of Λ–S states

The lowest 7 Λ–S electronic states of CdH^+, $X^1\Sigma^+$, $1^3\Sigma^+$, $A^1\Sigma^+$, $1^1\Pi$, $1^3\Pi$, $3^1\Sigma^+$, $2^3\Sigma^+$, which are related to the dissociation limits of $Cd^+(^2S_g) + H(^2S_g)$, $Cd(^1S_g) + H^+(^1S_g)$, and $Cd^+(^2P_u) + H(^2S_g)$, were calculated using the MRCI + Q method with aug-cc-pwCVTZ-DK and aug-cc-pV5Z-DK basis set for Cd and H respectively. Fig. 1 shows the calculated PECs of the Λ–S states. The calculating step length was set at 0.05 Å for $R = 0.9$–4.0 Å and 0.1 Å for $R = 4.0$–6.0 Å in calculations of the single point energy of these electronic states. Except for the $A^1\Sigma^+$ state, which corresponds to the dissociation products of H^+ and neutral Cd atoms, all the other states are dissociated into ionic Cd^+ and neutral H atoms. As shown in Fig. 1, the two triplet Σ^+ states are pure repulsive states while the $1^3\Pi$ state is a bound state with potential well of 0.85 eV. On the other hand, all the four singlet states are bound or quasi-bound states. Each of the $X^1\Sigma^+$, $A^1\Sigma^+$ and $1^1\Pi$ states has a global energy minimum at the corresponding equilibrium bond distance R_e. The $3^1\Sigma^+$ state, however, has a local minimum around $R = 3.19$ Å, where an avoided crossing occurs between the $3^1\Sigma^+$ and $A^1\Sigma^+$ states. Because of the avoided crossing, the PEC of the $A^1\Sigma^+$ state has a barrier of 430 cm^{-1} at $R = 3.19$ Å (R_{ACP}), and that of the

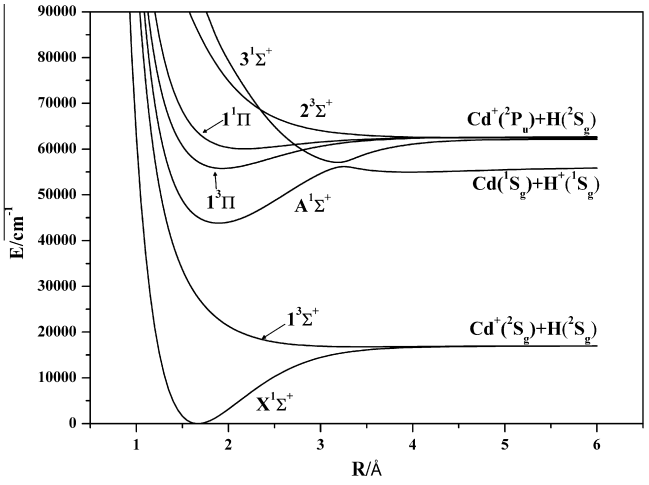

Fig. 1. The calculated PECs of the Λ–S states of CdH^+ using MRCI + Q method.

Table 1
The spectroscopic constants of the Λ–S state.

Λ–S state	T_e/cm^{-1}	R_e/Å	ω_e/cm^{-1}	$\omega_e\chi_e$/cm^{-1}	B_e/cm^{-1}	D_e/eV	Main electronic configuration (%)
$X^1\Sigma^+$	0	1.6660	1789.06	42.59	6.078	2.11	$10\sigma^2 11\sigma^0 12\sigma^0 6\pi^0$(69.3)
							$10\sigma^\alpha 11\sigma^\beta 12\sigma^0 6\pi^0$(22.1)
Expt.	0	1.6672[a]	1772.5[a]	35.40[a]	6.071[a]	2.18[a]	
Expt.	0	1.68[b]	1775[b]			2.12 ± 0.39[b]	
Calc.	0	1.808(1.931)[c]				1.469(1.524)[c]	
Calc.	0	1.74(1.78)[d]	1669(1665)[d]			2.12(1.99)[d]	
Calc.	0	1.70[e]	1690[e]			1.86[e]	
Calc.	0	1.709[f]	1696[f]			1.93[f]	
Calc.	0	1.709[g]	1672[g]	35.3[g]		1.908[g]	
Calc.	0	1.652[h]	1819.6[h]		6.232[h]	2.1767[h]	
Calc.	0	1.656[h]	1824.7[h]		6.200[h]	2.2212[h]	
$A^1\Sigma^+$	43801	1.895	1253.89	16.12	4.713	1.49	$10\sigma^\alpha 11\sigma^\beta 12\sigma^0 6\pi^0$(51.1)
							$10\sigma^\alpha 11\sigma^0 12\sigma^\beta 6\pi^0$(26.9)
							$10\sigma^2 11\sigma^0 12\sigma^0 6\pi^0$(21.1)
Expt.	42934.1[a]	1.8651[a]	1252[a]	8.6[a]	6.071[a]		
$1^3\Pi$	55767	1.935	1075.61	40.58	4.51	0.85	$10\sigma^\alpha 11\sigma^0 12\sigma^0 6\pi^\alpha$(92.7)
$1^1\Pi$	60070	2.171	691.62	45.80	3.58	0.32	$10\sigma^\alpha 11\sigma^0 12\sigma^0 6\pi^\beta$(90.8)
							$10\sigma^0 11\sigma^\alpha 12\sigma^0 6\pi^\beta$(1.5)
$3^1\Sigma^+$	57061	3.188	1326.97	86.95	1.67	0.63	$10\sigma^0 11\sigma^2 12\sigma^0 6\pi^0$(63.5)
							$10\sigma^\alpha 11\sigma^0 12\sigma^\beta 6\pi^0$(17.3)
							$10\sigma^2 11\sigma^0 12\sigma^0 6\pi^0$(6.5)
							$10\sigma^0 11\sigma^0 12\sigma^2 6\pi^0$(2.3)
							$10\sigma^0 11\sigma^0 12\sigma^0 6\pi^{\alpha\beta}$(2.1)

[c,d] Figures in parentheses are nonrelativistic results.
[a] Reference [23].
[b] Reference [24].
[c] Reference [25].
[d] Reference [26].
[e] Reference [27].
[f] Reference [28].
[g] Reference [29].
[h] Reference [30].

$3^1\Sigma^+$ state holds a shallow potential well of 0.63 eV. The energy gap of the two states at R_{ACP} was calculated to be 960 cm^{-1}. Such avoided crossing phenomenon as well as the spin–orbit interactions between the Λ–S states will be discussed in detail in the following section.

For the bound Λ–S states, the spectroscopic constants are calculated, including adiabatic transition energy (T_e), equilibrium bond distance (R_e), harmonic vibrational frequency (ω_e), anharmonic constant ($\omega_e\chi_e$), rotational constant (B_e) and dissociation energy (D_e). The results are presented in Table 1 along with the dominated electronic configurations at R_e of each state. For comparison, the available experimental and calculational results in the literatures are also listed in the table.

As shown in Table 1, all the electronic states of CdH^+ exhibit obvious multi-configuration character, thus it is expected that single-configuration methods could not give accurate results of the structure and spectroscopic constants of the states without enough correlation energy. Previous theoretical studies are only available for the ground $X^1\Sigma^+$ state of CdH^+, which are composed of two electronic configurations of $10\sigma^2 11\sigma^0 12\sigma^0 6\pi^0$ and $10\sigma^\alpha 11\sigma^\beta 12\sigma^0 6\pi^0$. Indeed, the MRCI + Q results are in good agreement with those obtained by multi-configuration CASPT2 calculation [30],

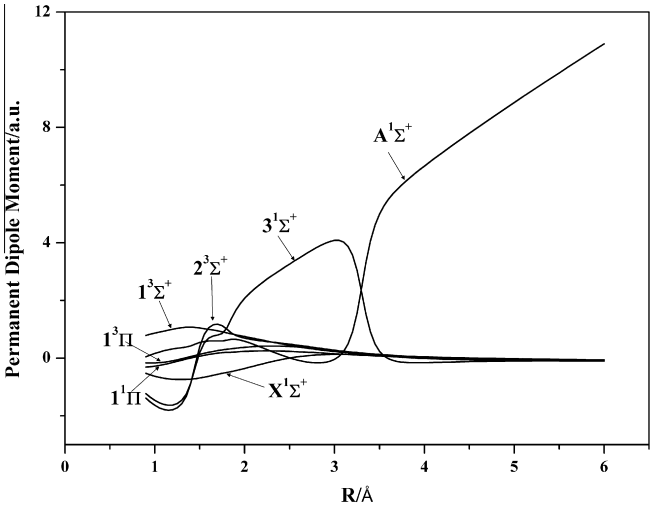

Fig. 2. The calculated Permanent dipole moments of the Λ–S states of CdH^+ as a function of the bond distance.

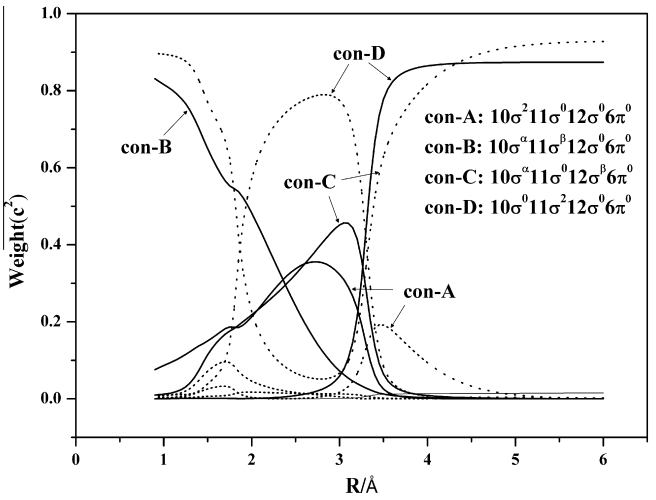

Fig. 3. The *R*-dependent weights c^2 of the dominated electronic configurations of the $A^1\Sigma^+$ state (solid lines) and the $3^1\Sigma^+$ state (dot lines).

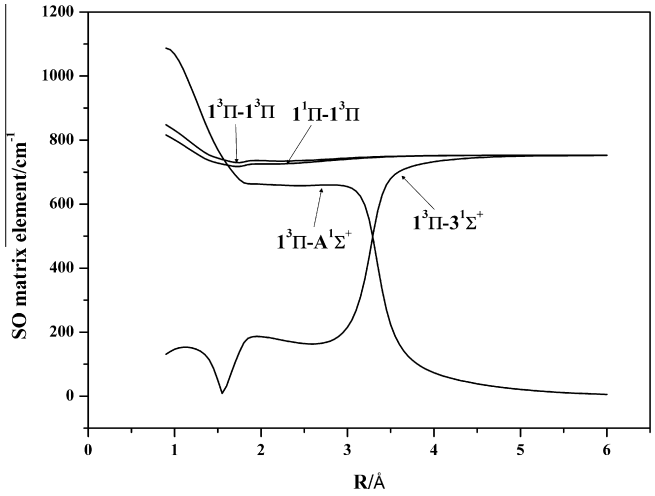

Fig. 4. The absolute R-dependent SO matrix elements of the Λ–S states.

Table 2
The dissociation limits of the Ω states.

Ω state	Atomic state	Energy	
$X0^+$, $(1)0^-$, (1)1	$Cd^+(^2S_{1/2}) + H(^2S_{1/2})$	0	0[a]
$(2)0^+$	$Cd(^1S_0) + H^+(^1S_0)$	38511	37139[a]
$(3)0^+$, $(2)0^-$, (2)1	$Cd^+(^2P_{1/2}) + H(^2S_{1/2})$	44084	44136[a]
$(4)0^+$, $(3)0^-$, (3)1, (4)1, (1)2	$Cd^+(^2P_{3/2}) + H(^2S_{1/2})$	46506	46619[a]

[a] Reference [41].

and those by CCSD (T) method [30] which could include high-level electron correlations. Other single-configuration calculations [25–29], however, have relatively large deviations. The high-level MRCI + Q calculation also supports the results from the early experimental studies [23,24], both for the ground $X^1\Sigma^+$ state and the excited $A^1\Sigma^+$ state. Regarding the electronic states with energy higher than the $A^1\Sigma^+$ state, to the best of the knowledge, there are neither theoretical nor experimental studies reported in the literature. The presented MRCI + Q calculations provide an accurate prediction of the spectroscopic constants, which thus would lead to future experimental studies on the excited electronic states of CdH^+.

Fig. 2 shows the permanent dipole moments (PDMs) of the seven Λ–S states of CdH^+ as a function of bond distance in the range of 0.9–6 Å, which were calculated using the MRCI method. As shown in Fig. 2, the value as well as the sign of the PDM of each state changes as the bond distance is increased. At large distance, the PDMs of the states exhibit two asymptotic limit because of the dissociation limits Cd + H^+ and Cd^+ + H of the CdH^+ cation. In detail, except for that of the $A^1\Sigma^+$ state, all the calculated PDMs lead to consistent asymptotic limit close to 0 a.u. because of the center of positive charges with the position vector $|\lambda| \approx 0$, which is corresponding to the dissociation limit of Cd^+ + H. The PDM of the $A^1\Sigma^+$ state, is positive and shows linear dependence on R at large bond distance because of the center of positive charges with the position vector $|\lambda| \approx R$, demonstrating that the dissociation limit of the $A^1\Sigma^+$ state is Cd + H^+ instead. It is interesting to see a pair of complementary abrupt change of the PDMs of the $A^1\Sigma^+$ state and the $3^1\Sigma^+$ state around the bond distance of R_{ACP}. Such abrupt change of the PDMs could be attributed to the change of

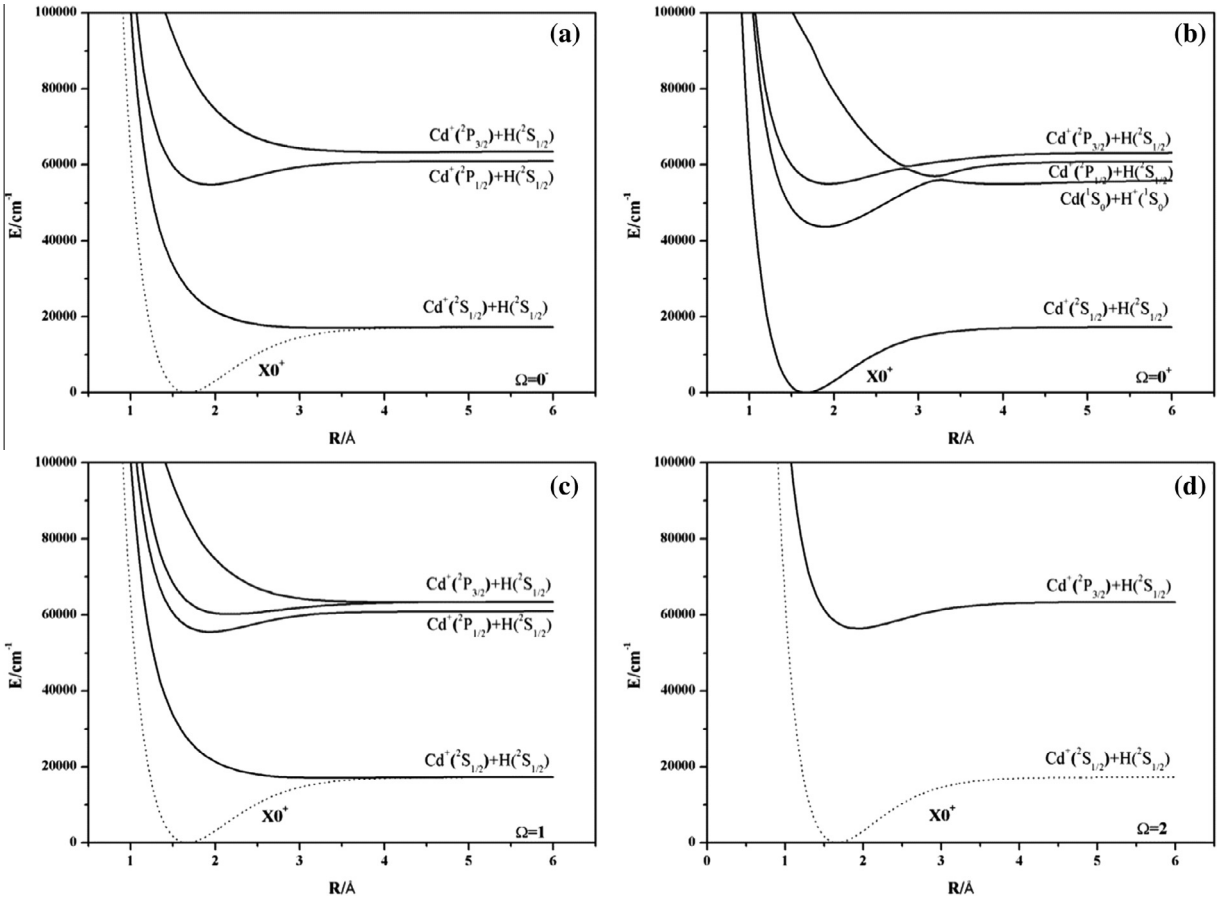

Fig. 5. The PECs of the Ω states (a) Ω = 0^-, (b) Ω = 0^+, (c) Ω = 1, and (d) Ω = 2.

Table 3
The spectroscopic constants of the Ω state.

Ω state	T_e/cm^{-1}	R_e/Å	ω_e/cm^{-1}	$\omega_e\chi_e$/cm^{-1}	B_e/cm^{-1}	D_e/eV	Dominant Λ–S composition at R_e (%)
X0$^+$	0	1.6650	1775.49	40.73	6.079	2.15	$X^1\Sigma^+$(100)
Expt.	0	1.6672[a]	1772.5[a]	35.40[a]	6.071[a]	2.18[a]	
Expt.	0	1.68[b]	1775[b]			2.12 ± 0.39[b]	
(2)0$^+$	43655	1.8940	1255.20	16.69	4.715	1.51	$A^1\Sigma^+$(99.1), $^3\Pi$(0.9)
Expt.	42934.1[a]	1.8651[a]	1252.0[a]	8.6[a]	6.071[a]		
(2)0$^-$	54789	1.9335	1083.65	45.04	4.511	0.76	$^3\Pi$(99.8), $^3\Sigma^+$(II)(0.2)
(3)0$^+$	54924	1.9295	1023.37	30.00	4.529	0.73	$^3\Pi$(99.1), $A^1\Sigma^+$(0.9)
	56949[c]	3.1950[c]	1455.34[c]	–	1.688[c]	0.48[c]	$3^1\Sigma^+$ (96.8), $A^1\Sigma^+$(1.6), $^3\Pi$(1.5)
(2)1	55475	1.9380	1026.99	40.47	4.496	0.67	$^3\Pi$(97.6), $^1\Pi$(2.3)
(1)2	56416	1.9305	1089.36	41.16	4.526	0.86	$^3\Pi$(100)
(4)0$^+$	59503	2.8620	1045.32	82.44	2.068	0.45	$^3\Pi$(56.7), $^1\Sigma^+$(III)(42.0), $A^1\Sigma^+$(1.4)
(3)1	60187	2.1630	720.89	37.95	3.612	0.39	$^1\Pi$(95.6), $^3\Pi$(4.1), $^3\Sigma^+$(II)(0.3)

[a] Reference [23].
[b] Reference [24].
[c] Spectroscopic constants obtained from external well.

the wavefunctions of the two electronic states around their avoided crossing region. To clarify this, it is presented in Fig. 3 the R-dependent weights c^2 of the $A^1\Sigma^+$ and the $3^1\Sigma^+$ state, where c is the coefficient of the dominated electronic configurations (con-A, -B, -C,-D) of the states. As indicated in the figure, the con-B plays an important role in the $A^1\Sigma^+$ state at short distance, but reduces quickly before R_{ACP}. The main configurations involved in the wavefunctions of the $A^1\Sigma^+$ and $3^1\Sigma^+$ states around R_{ACP} are con-A, con-C, and con-D. The weight (c^2) of each configuration presents a pair of abrupt changes at R_{ACP}, respectively. In other words, the main electronic configurations for the $A^1\Sigma^+$ and $3^1\Sigma^+$ states are exchanged through R_{ACP}, which represents the changes on wavefunctions of the $A^1\Sigma^+$ and $3^1\Sigma^+$ states, thus leading to the abrupt changes of the PDMs in the avoided crossing region.

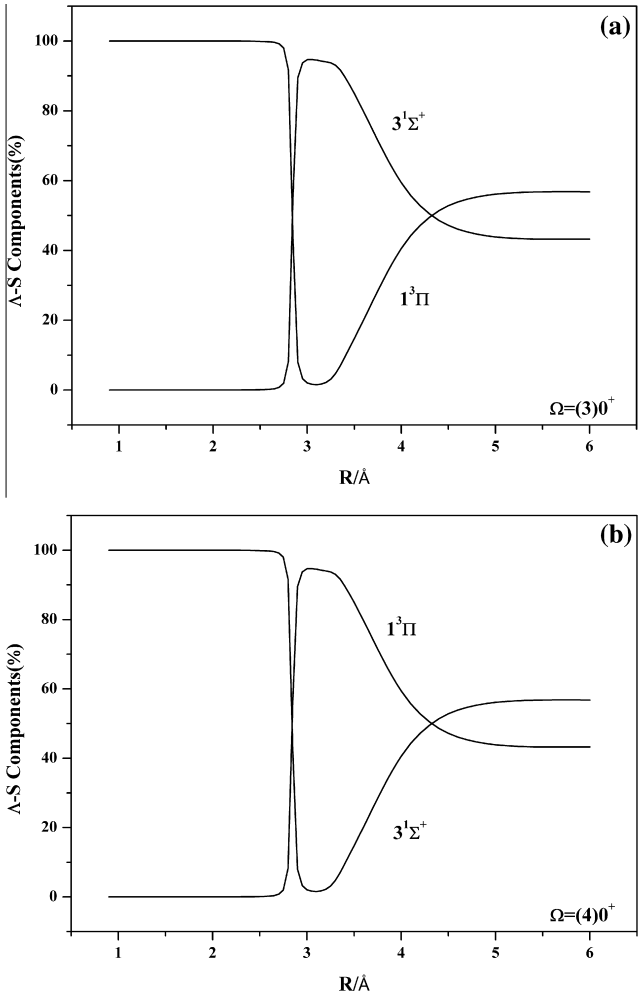

Fig. 6. The Λ–S compositions of 0$^+$ states (a) Ω = (3)0$^+$ and (b) Ω = (4)0$^+$.

3.2. The PECs and spectroscopic constants of Ω states

Spin–orbit coupling effect leads to the strong interaction for Λ–S states of the molecules containing heavy elements. Especially at the intersections of PECs, under the influence of strong interaction, the perturbations between the interacting electronic states may result. The quantitative evaluation of the interaction depends on the spin–orbit matrix element. The spin–orbit matrix element of the five excited Λ–S states of CdH^+ with transition energies larger than 40,000 cm^{-1} were calculated. The $3^1\Sigma^+$–$1^1\Pi$ and $3^1\Sigma^+$–$2^3\Sigma^+$ pairs have no common Ω components, thus no interactions by SOC effect could result. Fig. 4 shows the R-dependent spin–orbit coupling matrix elements of the system $1^3\Pi$–$1^3\Pi$, $1^3\Pi$–$1^1\Pi$, $A^1\Sigma^+$–$1^3\Pi$ and $3^1\Sigma^+$–$1^3\Pi$ at bond distances of 0.9–6.0 Å. It could be observed that all the SO matrix elements converge to two different limits. The one from the SO interaction of 5p orbital is about 770 cm^{-1}, while the other one is equal to 0 cm^{-1}, because there is no SOC between 5s and 5p orbitals. Both $1^3\Pi$ and $1^1\Pi$ states have the same electronic configuration of $10\sigma^1 11\sigma^0 12\sigma^0 6\pi^1$ over the internuclear distance. The SO matrix elements of $1^3\Pi$–$1^3\Pi$ and $1^3\Pi$–$1^1\Pi$ remain almost

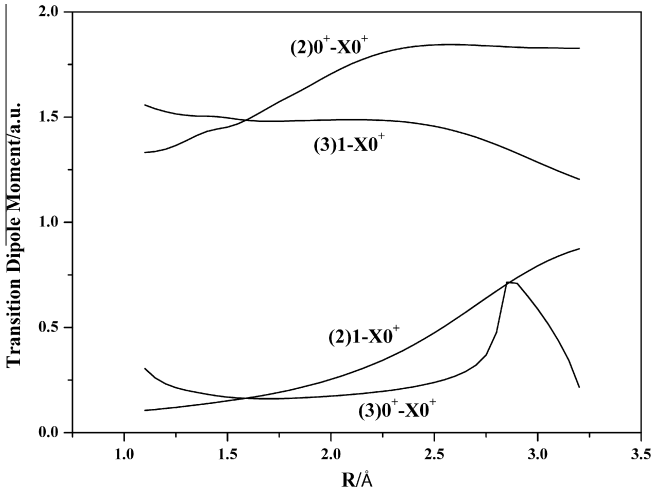

Fig. 7. The Transition dipole moments of the transitions from (2)0$^+$, (3)0$^+$, (2)1, and (3)1 to X0$^+$.

Table 4
Radiative lifetimes of the transitions from $(2)0^+$, $(3)0^+$, (2)1, and (3)1 to ground $X0^+$ state.

Transition	Radiative lifetimes (ns)							
	$v'=0$	$v'=1$	$v'=2$	$v'=3$	$v'=4$	$v'=5$	$v'=6$	$v'=7$
$(2)0^+ - X0^+$	2.68	2.71	2.74	2.76	2.78	2.79	2.81	2.84
$(3)0^+ - X0^+$	94.66	97.90	101.45	104.65	109.58			
$(2)1 - X0^+$	24.37	25.28	26.25	27.35	28.69	30.42	32.82	
$(3)1 - X0^+$	1.41	1.47	1.55	1.63	1.72			

unchanged as R is increased, of which the numerical values are about 770 cm^{-1} over Cd–H distance. It could be noticed that the abrupt changes of the electronic configurations in wavefunctions for the $A^1\Sigma^+$ and $3^1\Sigma^+$ states also bring large influence to the related SO matrix elements. Just like the phenomenon observed in the PDMs of the $A^1\Sigma^+$ and $3^1\Sigma^+$ states (Fig. 2), the SO matrix elements of $A^1\Sigma^+$–$1^3\Pi$ and $3^1\Sigma^+$–$1^3\Pi$ also encounter a pair of complementary sudden changes around R_{ACP}.

After considering the SOC effect, the original 7 Λ–S states are split into 12 Ω states including three $\Omega=0^-$ states, four $\Omega=0^+$ states, four $\Omega=1$ states, and one $\Omega=2$ state. The dissociation limits $Cd^+(^2S_g)+H(^2S_g)$, $Cd(^1S_g)+H^+(^1S_g)$, and $Cd^+(^2P_u)+H(^2S_g)$ yield four new asymptotes $Cd^+(^2S_{1/2})+H(^2S_{1/2})$, $Cd(^1S_0)+H^+(^1S_0)$, $Cd^+(^2P_{1/2})+H(^2S_{1/2})$, and $Cd^+(^2P_{3/2})+H(^2S_{1/2})$. The relationships between the Ω states and the dissociation limits are listed in Table 2. The calculated spin–orbit atomic states are in good agreement with the measured values reported in the literature. [41]. Fig. 5 shows the calculated PECs for (a) $\Omega=0^-$, (b) $\Omega=0^+$, (c) $\Omega=1$ and (d) $\Omega=2$ states respectively. In each figure, the PEC of the ground state is also presented for comparison.

As shown in Fig. 5, four of the 12 Ω states are pure repulsive states, i.e., $(1)0^-$, $(3)0^-$, (1)1 and (4)1 states. These Ω states are spin–orbit split from the two repulsive $^3\Sigma^+$ states. Because of no crossing with the other states, each $^3\Sigma^+$ is split into one $\Omega=0^-$ and one $\Omega=1$ state that remain repulsive. Based on the computed Ω-state PECs, the spectroscopic constants of the CdH^+ are numerically obtained, which are listed in Table 3. The dominant Λ–S composition at R_e of each Ω state are also listed in the table. The ground state $X0^+$ is composed of 100% $X^1\Sigma^+$ Λ–S state; hence, the spectroscopic parameters of $X0^+$ given in Table 3 are almost the same as those of the Λ–S ground state $X^1\Sigma^+$. Under the SOC effect, a Λ–S state will be split into different Ω states. The states with the same Ω could lead to strong SOC, thus the avoided crossing in the PECs. This is particularly significant in the PECs of the excited $\Omega=0^+$ states. As shown in Fig. 5(b), two apparent avoided crossings could be observed at $R=2.82$ Å and $R=3.19$ Å. The latter is attributed to the avoided crossing between the $A^1\Sigma^+$ and the $3^1\Sigma^+$ states as discussed in the previous section. The avoided crossing at $R=2.82$ Å between $(3)0^+$ and $(4)0^+$ states is the result of the SOC effect. Thus after considering the SOC effect, the computed spectroscopic constants of the Ω states in Table 3 would be quite different from those for the pure Λ–S states in Table 1. To further illustrate the SOC effect and the resulting avoided crossing of the PECs, it is presented in Fig. 6 the R-dependent compositions of the Λ–S states of $(3)0^+$ and $(4)0^+$ states in the range of 0.9–6 Å. As shown in the figure, the Λ–S state compositions for the Ω states switch between the $3^1\Sigma^+$ and the $1^3\Pi$ states around the internuclear distance where the crossings occurs, strongly indicate the coupling between the states.

3.3. The analysis of the transition properties

The absolute transition dipole moments (TDMs) from the ground $X0^+$ state to the excited Ω states, $(2)0^+$, $(3)0^+$, (2)1 and (3)1 were calculated as a function of the internuclear distance, as depicted in Fig. 7. In the Franck–Condon region, the transitions of $(2)0^+ - X0^+$ and $(3)1 - X0^+$ have much larger TDMs due to result from the spin-allowed transitions $A^1\Sigma^+$–$X^1\Sigma^+$ and $1^1\Pi$–$X^1\Sigma^+$, respectively. The remaining transitions $(3)0^+ - X0^+$ and $(2)1 - X0^+$, on the contrary, arise from the spin-forbidden $1^3\Pi$–$X^1\Sigma^+$ and $2^3\Sigma^+$–$X^1\Sigma^+$ transitions and thus have smaller TDMs. The (2)1 state is nearly composed of $1^3\Pi$ at the small R. However, the $^1\Pi$ component plays the more and more important role in the (2)1 state with increasing R (see Fig. S1 in the Supplementary Materials). In particular, when $R>3.5$ Å, the percentage of weight for the $^1\Pi$ state become as much as 30%. In addition, the transition $^1\Pi$–$X^1\Sigma^+$ belongs to the spin-allowed transition and have larger TDM. All of these could explain that why the TDM curve of (2)1 has the increasing TDM rather than zero. It can also be seen from Fig. 7 that the TDM of the transition $(3)0^+ - X0^+$ is characterized by a peak at the internuclear distance of 2.85 Å, where the avoided crossing between the $(3)0^+$ and $(4)0^+$ states occurs. This could be explained by the aforementioned sudden change of main Λ–S state components of the $(3)0^+$ state from the spin-forbidden $1^3\Pi$ state to the spin-allowed $3^1\Sigma^+$ state around the avoided crossing point (see Fig. 6). The results indicate that the SOC effect plays an important role in the PECs, the spectroscopic constants as well as the transition properties of the low-lying states of CdH^+ cation.

Based on the calculated TDMs, the radiative lifetime of the selected vibrational level v' has been computed by the following formula [42,43].

$$\tau_{v'} = (A_{v'})^{-1} = \frac{3h}{64\pi^4 \left|a_0 \cdot e \cdot \overline{TDM}\right|^2 \sum_{v''} q_{v',v''} (\Delta E_{v',v''})^3} = \frac{4.936 \times 10^5}{\left|\overline{TDM}\right|^2 \sum_{v''} q_{v',v''} (\Delta E_{v',v''})^3}$$

where $q_{v',v''}$ is the Franck–Condon factor(see Table S1 in the Supplementary Materials), $\overline{TDM}$ is the averaged transition dipole moment in atomic unit, the energy separation $\Delta E_{v',v''}$ is in cm^{-1}, and $\tau_{v'}$ is in second. The results are shown in Table 4. The computed radiative lifetimes of the $(3)0^+$ and (2)1 states are in the order of ten nanoseconds and those of the $(2)0^+$ and (3)1 states are in the order of one nanoseconds. Since the four transitions have comparable Franck–Condon factors and the energy separations while the $(3)0^+ - X0^+$ transition has the smallest TDM in the Franck–Condon region, the radiative lifetimes of the $(3)0^+ - X0^+$ transition are expected to be the largest, as indicated in the results in Table 4.

4. Conclusions

The relativistic MRCI + Q calculations on the ground and low-lying excited states of CdH^+ have been carried out. The PECs of seven Λ–S states are plotted with the aid of the avoided crossing rule, from which, the corresponding spectroscopic constants are derived. The analysis of the wavefunctions shows that the Λ–S states, especially the $A^1\Sigma^+$ state, are multi-configurational in nature. The PDMs of the seven Λ–S states are calculated at $R=0.9$–6.0 Å. Because of the different dissociation limits $Cd + H^+$ and $Cd^+ + H$ at large distance, the PDMs are linear approximation of R a.u. for $A^1\Sigma^+$ state, while being 0 a.u. for the remaining Λ–S states. The abrupt changes of the PDMs ($A^1\Sigma^+$ and $3^1\Sigma^+$) and the SO

matrix elements ($A^1\Sigma^+$–$1^3\Pi$ and $3^1\Sigma^+$–$1^3\Pi$) reveal the sharp changes for the electron configurations in the wavefunctions of $A^1\Sigma^+$ and $3^1\Sigma^+$ at their avoided crossing point. Taking consideration of the SOC effect, 12 Ω states which are generated from the Λ–S states were investigated. The transition properties of $(2)0^+ - X0^+$, $(3)0^+ - X0^+$, $(2)1 - X0^+$, and $(3)0^+ - X0^+$ are reported, including the transition dipole moments, Franck–Condon factors, and radiative lifetimes. This study indicates that SOC effect exhibits great influence on the PECs, the spectroscopic constants as well as the transition properties of the low-lying states of CdH^+ cation.

Conflict of interest

There is no conflict of interest.

Acknowledgement

This work was supported by National Natural Science Foundation of China (11274140). The High Performance Computing Center (HPCC) of Jilin University for supercomputer time is acknowledged.

Appendix A. Supplementary data

Supplementary data associated with this article can be found, in the online version, at http://dx.doi.org/10.1016/j.chemphys.2014.09.003.

References

[1] G.L. Soloveichik, B.M. Bulychev, Russ. Chem. Rev. 52 (1983) 43.
[2] R.G. Pearson, Chem. Rev. 85 (1985) 41.
[3] H. Smithson, C.A. Marianetti, D. Morgan, A. Van der Ven, A. Predith, G. Ceder, Phys. Rev. B 66 (2002) 144107.
[4] R.S. Mulliken, Proc. Natl. Acad. Sci. 12 (1926) 151.
[5] R.S. Mulliken, Phys. Rev. 32 (1928) 388.
[6] G. Stenvinkel, E. Svensson, Nature 135 (1935) 955.
[7] M.A. Khan, Proc. Phys. Soc. 80 (1962) 1264.
[8] A. Jourdan, J.M. Negre, J. Dufayard, O. Nedelec, J. Phys. Lett. 37 (1976) 29.
[9] W.J. Balfour, Phys. Scr. 25 (1982) 257.
[10] W.J. Balfour, R.S. Ram, J. Mol. Spectrosc. 121 (1987) 199.
[11] O. Nedelec, B. Majournat, J. Dufayard, Chem. Phys. 134 (1989) 137.
[12] A. Avramopoulos, V.E. Ingamells, M.G. Papadopoulos, A.J. Sadlej, J. Chem. Phys. 114 (2001) 198.
[13] W.L. Zou, W.J. Liu, J. Comput. Chem. 28 (2005) 2286.
[14] A. Shayesteh, R.J. Le Roy, T.D. Varberg, P.F. Bernath, J. Mol. Spectrosc. 237 (2006) 87.
[15] R. Li, Z. Zhai, X.M. Zhang, M.X. Jin, H.F. Xu, B. Yan, Chem. Phys. Lett. 599 (2014) 51.
[16] J.B. Schilling, W.A. Goddard III, J.L. Beauchamp, J. Phys. Chem. 91 (1987) 5616.
[17] J.B. Schilling, W.A. Goddard III, J.L. Beauchamp, J. Am. Chem. Soc. 108 (1986) 582.
[18] N.S. Mosyagin, A.V. Titov, E. Eliav, U. Kaldor, J. Chem. Phys. 115 (2001) 2007.
[19] T.K. Ghanty, E.R. Davidson, Int. J. Quantum Chem. 77 (2000) 291.
[20] M. Filatov, D. Cremer, Chem. Phys. Lett. 351 (2002) 259.
[21] C.R. Williams, R.M. Harrison, Experientia 40 (1984) 29.
[22] J.M. Bewers, P.J. Barry, D.J. MacGregor, Adv. Environ. Sci. Technol. 19 (1987) 1.
[23] K.P. Huber, G. Herzberg, Molecular Spectra and Molecular Structure IV: Constants of Diatomic Molecules, Van Nostrand Reinhold, New York, 1979.
[24] K.S. Krasnov, V.S. Timoshinin, T.G. Danilova, S.V. Khandozhko, Handbook of Molecular Constants of Inorganic Compounds, Israel Program for Scientific Translations, Jerusalem, 1970.
[25] P. Pyykkö, J. Chem. Soc. Faraday Trans. II (75) (1979) 1256.
[26] T. Ziegler, J.G. Snijders, E.J. Baerends, J. Chem. Phys. 74 (1981) 1271.
[27] D. Strömberg, O. Gropen, U. Wahlgren, Chem. Phys. 133 (1989) 207.
[28] J.B. Schilling, W.A. Goddard III, J.L. Beauchamp, J. Am. Chem. Soc. 109 (1987) 5565.
[29] E. Eliav, U. Kaldor, B.A. Hess, J. Chem. Phys. 108 (1998) 3409.
[30] M. Abe, M. Kajita, M. Hada, Y. Moriwaki, J. Phys, Mol. Opt. Phys. 43 (2010) 245102.
[31] H.-J. Werner, P.J. Knowles, et al., MOLPRO, a package of ***ab initio*** programs, Version 2010, <http://www.molpro.net>.
[32] R.J. Le Roy, LEVEL 8.0: A Computer Program for Solving the Radial Schrödinger Equation for Bound and Quasibound Levels, University of Waterloo Chemical Physics Research Report CP-663 2007.
[33] K.A. Peterson, D. Figgen, M. Dolg, H. Stoll, J. Chem. Phys. 126 (2007) 124101.
[34] T.H. Dunning, J. Chem. Phys. 90 (1989) 1007.
[35] H.-J. Werner, P.J. Knowles, J. Chem. Phys. 82 (1985) 5053.
[36] P.J. Knowles, H.-J. Werner, Chem. Phys. Lett. 115 (1985) 259.
[37] H.-J. Werner, P.J. Knowles, J. Chem. Phys. 89 (1988) 5803.
[38] P.J. Knowles, H.-J. Werner, Chem. Phys. Lett. 145 (1988) 514.
[39] M. Douglas, N.M. Kroll, Ann. Phys. 82 (1974) 89.
[40] A. Berning, M. Schweizer, H.-J. Werner, P.J. Knowles, P. Palmieri, Mol. Phys. 98 (2000) 1823.
[41] C.E. Moore, Atomic Energy Levels, National Bureau of Standards, Washington, DC, 1971.
[42] H. Okabe, Photochemistry of Small Molecules, Wiley-Interscience, New York, 1978.
[43] W.L. Zou, W.J. Liu, J. Comput. Chem. 26 (2005) 106.